

## Asymptotic densities of ballistic Lévy walks

D. Froemberg,<sup>1</sup> M. Schmiedeberg,<sup>2</sup> E. Barkai,<sup>3</sup> and V. Zaburdaev<sup>1</sup>

<sup>1</sup>Max Planck Institute for the Physics of Complex Systems, Nöthnitzer Str. 38, D-01187 Dresden, Germany

<sup>2</sup>Institut für Theoretische Physik 2: Weiche Materie, Heinrich-Heine-Universität Düsseldorf, 40204 Düsseldorf, Germany

<sup>3</sup>Department of Physics, Institute of Nanotechnology and Advanced Materials, Bar-Ilan University, Ramat-Gan, 52900, Israel

(Received 2 December 2014; published 20 February 2015)

We propose an analytical method to determine the shape of density profiles in the asymptotic long-time limit for a broad class of coupled continuous-time random walks which operate in the ballistic regime. In particular, we show that different scenarios of performing a random-walk step, via making an instantaneous jump penalized by a proper waiting time or via moving with a constant speed, dramatically effect the corresponding propagators, despite the fact that the end points of the steps are identical. Furthermore, if the speed during each step of the random walk is itself a random variable, its distribution gets clearly reflected in the asymptotic density of random walkers. These features are in contrast with more standard nonballistic random walks.

DOI: [10.1103/PhysRevE.91.022131](https://doi.org/10.1103/PhysRevE.91.022131)

PACS number(s): 05.40.Fb, 45.50.-j

### I. INTRODUCTION

Ballistic motion is ubiquitous and often lies at the origin of stochastic transport phenomena. Swimming bacterial cells, scattered photons, or atoms in optical lattices [1–8] move with fixed speeds between tumbles and collisions which reset their velocities to new values and eventually lead to the randomization of the dispersal process. However, there is a large class of diffusion processes where the ballistic behavior of particles between the reorientation events is retained at larger scales [3,9–11]. Such ballistic diffusion processes can be modelled on the stochastic level by certain classes of random walks, the so-called Lévy walks, where the displacements and the time intervals between the successive direction renewals are coupled [12–15]. What all these ballistic random walks do have in common is that the probability density function (pdf) of the time intervals has a slowly decaying power-law tail  $\psi(\tau) \propto t^{-1-\gamma}$  with  $0 < \gamma < 1$ . This pdf lacks a typical scale (has a divergent mean) and gives rise to the ballistic scaling of the whole density profile of diffusing particles. Depending on the implementation of the space-time coupling one has to distinguish between jump and velocity models [16]. In velocity models a particle moves at a certain random but constant velocity during the flight time and at each renewal a new velocity and a new flight time are chosen from the corresponding probability distributions. In the jump models [17], the displacement of the particle takes place instantaneously but is penalized by a certain waiting time—longer jumps will require longer waiting before another jump may occur. In the wait-first model the particle jumps at the end of the waiting time, whereas in the jump-first model the particle jumps and then rests for the corresponding waiting time. Such random walks were previously considered in the literature [18–26] and recently also with a method of infinite densities [27] in the sub-ballistic superdiffusive regime (flight or waiting times with finite mean,  $1 < \gamma < 2$ ). However, in general the exact analytical solutions describing the density of random walking particles are rare and can be obtained only for some particular values of  $\gamma$  [16,28].

In this paper we suggest a method to compute explicitly the asymptotic densities of random walks in the regime of ballistic scaling. We show that this approach can be applied

both to coupled jump models and to the models with random velocities, the latter being related to weak ergodicity breaking. Remarkably, the choice of whether the particle jumps at the beginning or end of the waiting time (jump models), as well as the distribution of velocities (velocity models) has a dramatic effect on the shape of the particles' density, a result which could not be obtained from the standard asymptotic analysis routinely employed in random walks.

### II. MODELS

Let us briefly recap the basic microscopic equations of the models considered in the present paper. Here we restrict ourselves to the one-dimensional case. In the jump models the jumps are penalized by a waiting time. For the jump-first model, the particle performs a jump according to a jump-length pdf  $f(x)$  and then waits for a time  $\tau$  drawn from an  $x$ -dependent waiting-time pdf  $\psi(\tau|x)$ . This process is then renewed. For the wait-first model, the particle waits first for a time  $\tau$  drawn from the waiting-time pdf  $\psi(\tau)$  and then jumps over a distance  $x$  given by  $f(x|\tau)$  at the end of the waiting time (see Fig. 1). Thus it is easy to construct a balance equation for the probability density of particles  $Q_\alpha(x,t)$  to end a step at  $x$  at time  $t$  ( $\alpha = "j"$  or  $"w"$ , denoting jump- or wait-first models, respectively). The pdf that the step ends at  $x$  at time  $t$  is determined by the joint pdf  $K(x',\tau)$  that the actual jump had length  $x'$  and duration  $\tau$ , provided that the particle ended its previous jump at  $x - x'$  at  $t - \tau$ ,

$$Q_\alpha(x,t) = \int_{-\infty}^{\infty} dx' \int_0^t K_\alpha(x',\tau) Q_\alpha(x-x',t-\tau) d\tau + \delta(x)\delta(t). \quad (1)$$

Here the coupled jump kernels for each model are  $K_w = \psi(\tau)f(x'|\tau)$  and  $K_j = f(x')\psi(\tau|x')$ , and the last summand is the initial condition. Note that the distinction between the  $Q_\alpha$  at this point is only a formal one. The  $Q_\alpha$  are mathematically the same for both jump models. Still, both models qualitatively differ, and the  $K_\alpha$  contain the information about which variables are dependent or independent (and thus implicitly on what happens between the start and end of a jump) which comes into effect in the following equations for the

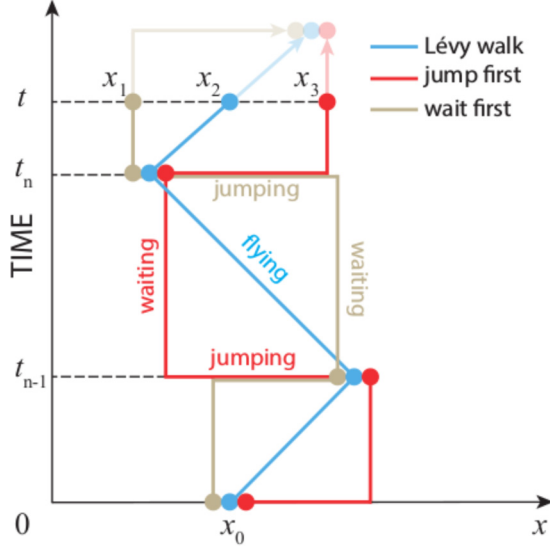


FIG. 1. (Color online) Trajectories of the three stochastic models investigated in the text. Lévy walk (blue), wait-first (green), and jump-first (red) models produce trajectories which take different paths but pass through the same end points on the  $(x, t)$  plane. Therefore, only the very last, uncompleted step distinguishes these three models.  $t_n$  is the last renewal event before the measurement time  $t$ , and  $t - t_n$  is called the backward recurrence time.

densities. We assume that the process starts at  $x = 0$  and  $t = 0$  so the beginning of the first waiting-time interval coincides for all sample trajectories. The expressions for the density of particles are then:

$$p_w(x, t) = \int_0^t \Psi(\tau) Q_w(x, t - \tau) d\tau, \quad (2)$$

$$p_j(x, t) = \int_{-\infty}^{\infty} dx' \int_0^t f(x') \Psi(\tau|x') Q_j(x - x', t - \tau) d\tau, \quad (3)$$

where  $\Psi(t) = 1 - \int_0^t \psi(\tau) d\tau$  and  $\Psi(\tau|x) = 1 - \int_0^\tau \psi(\tau'|x) d\tau'$  are the survival probabilities, which are equivalent to the probabilities that no renewal occurs up to time  $t$ .

The initial conditions for the jump-first model must be treated with some care. As stated in Eq. (1) at time  $t = 0$  the system is prepared and the particle is at the origin. We assume that a jump took place at  $t = 0^+$ . In that sense the process begins at the start of the measurement. Thus, if taking  $t \rightarrow 0^+$  one finds with Eq. (1) for the wait-first case Eq. (2)  $p_w(x, 0) = \delta(x)$  and for the jump-first case Eq. (3)  $p_j(x, 0) = f(x)$ , as expected.

In particular, we will look at the linear coupling for the jump models, meaning that the waiting time is linearly proportional to the jump distance. This results in the simple coupling functions [16]

$$f(x|\tau) = \delta(|x| - v_0\tau), \quad (4)$$

$$\psi(\tau|x) = \delta(\tau - v_0^{-1}|x|). \quad (5)$$

We denote the proportionality constant by  $v_0$  as it has the dimension of a velocity (and can indeed be considered as the speed of the single particle if one measures the ratio of the distance traveled to the duration of the step). The particular form of the primary waiting-time pdf  $\psi(\tau)$  and jump-length pdf  $f(x)$  will be specified later when needed. The following general considerations do not require such specification yet.

A different scenario is a velocity model (see Fig. 1), where during each step of duration  $\tau$  drawn from  $\psi(\tau)$  a particle moves with a constant speed  $v$  drawn according to a velocity pdf  $h(v)$ . Equivalently to the loss flux in the jump model, we now write down the balance equation for the probability density  $\nu(x, t)$ , which describes the frequency of velocity changes at point  $x$  at a given time  $t$ ,

$$\nu(x, t) = \int_{-\infty}^{\infty} dv \int_0^t \nu(x - v\tau, t - \tau) h(v) \psi(\tau) d\tau + \delta(x) \delta(t). \quad (6)$$

A velocity change can occur in  $x$  and at time  $t$  if the previous velocity change to the value  $v$  took place at  $x - v\tau$  at the time  $t - \tau$ . With this we get the particle density

$$p_\nu(x, t) = \int_{-\infty}^{\infty} dv \int_0^t \nu(x - v\tau, t - \tau) h(v) \Psi(\tau) d\tau, \quad (7)$$

where  $\Psi(\tau) = 1 - \int_0^\tau \psi(\tau') d\tau'$  is again the probability not to have a renewal until  $\tau$ .

Note that in the special case of the velocity model (Lévy walk) with just one speed  $h(v) = 1/2[\delta(v - v_0) + \delta(v + v_0)]$  [16,18,29] the starting points and end points of the consecutive steps coincide with those of the jump models with linear coupling, although the paths in the  $(x, t)$  plane differ (see Fig. 1). Therefore these models differ only by their last, incomplete step. As we proceed to show, this seemingly minor difference leads to dramatic effects on particles' pdf  $p(x, t)$ . Beyond the fundamental interest in the long-time limit of random walks, this issue is important also for computer-generated random walks, since, in the normal situation, these definitions of sample paths all converge to unique behavior.

### III. PROPAGATORS

#### A. General expressions in Fourier-Laplace space

Equations (1), (2), and (3) for the jump models and Eqs. (6) and (7) for the velocity model are solved with the help of Fourier-Laplace transforms [30]. By setting the initial distribution of particles to the  $\delta$  function  $p(x, t = 0) = \delta(x)$  we can find the propagators  $G(x, t)$  for all three models. For the jump models, in Fourier-Laplace domain we get [31] (see Appendix A):

$$G_j(k, s) = \frac{\mathcal{FL}\{f(x)\Psi(\tau|x)\}}{1 - \mathcal{FL}\{f(x)\psi(\tau|x)\}}, \quad (8)$$

$$G_w(k, s) = \frac{\mathcal{L}\{\Psi(\tau)\}}{1 - \mathcal{FL}\{f(x|\tau)\psi(\tau)\}}, \quad (9)$$

where  $\mathcal{F}$  and  $\mathcal{L}$  stand for Fourier and Laplace transforms, with  $k$  and  $s$  denoting the coordinates conjugate to  $x$  and  $t$ , respectively.

Using Eqs. (6) and (7) and convolution theorems for Fourier and Laplace transforms, we get in accordance with previous studies [28,32] the propagator of the velocity model  $G_v$  which is given by

$$G_v(k,s) = \frac{\mathcal{L}\{\Psi(\tau)h(k\tau)\}}{1 - \mathcal{L}\{\psi(\tau)h(k\tau)\}}, \quad (10)$$

where  $k\tau$  is the Fourier variable conjugate to  $v$  and hence the (spatial) Fourier transform of the velocity distribution  $\mathcal{F}\{h(v)\} = \int_{-\infty}^{\infty} e^{-ik\tau v} h(v) dv = h(k\tau)$ .

Equation (10) retains the form of the well-known Montroll-Weiss [33] equation for the pdf of the (uncoupled) continuous-time random walk (CTRW) to find the particle at  $x$  at time  $t$ , modified such that it applies to random jumps taking place not in space but in velocity [34]. Equation (9) is a special case of an equation for CTRW introduced by Scher and Lax [12], accounting for coupled waiting times and jump lengths. Equation (8) represents a further modification of the latter, reflecting the fact that there the survival probability  $\Psi(\tau|x)$  depends on the jump length.

The numerators in Eqs. (8) and (10) reflect the effect of the last jump interval in the process on the final position of the particle. This last incomplete time interval is called backward recurrence time  $\tau_b = t - t_n$ , where  $t_n$  is the epoch of the last renewal (see Fig. 2). As we will see later, this last interval has a crucial effect on the shape of the asymptotic particle pdfs, unlike usual random-walk theories. Note that, though in a slightly different manner, the statistics of the last jump event also plays an important role in the description of transport of cold atoms in optical lattices [35].

An analytical representation and a direct inversion of Eqs. (8) and (10) is not feasible in most cases. As an alternative, one has to resort to the asymptotic analysis for large space and time scales  $x, t \rightarrow \infty$ . Going to Fourier-Laplace space using the Tauberian theorem [14], this limit corresponds to  $(k,s) \rightarrow (0,0)$ , in our (ballistic) case such that  $(k/s) = \text{const}$ . However, even then the explicit analytical Fourier-Laplace inversion is often not possible and has to be performed numerically. In the following, we assume that the persistence time and jump-length pdfs fall off like a power law:

$$\psi(\tau) = \frac{1}{\tau_0} \frac{\gamma}{(1 + \tau/\tau_0)^{1+\gamma}}, \quad 0 < \gamma < 1, \quad (11)$$

for the waiting time of the wait-first model and for the flight time of the velocity model, and

$$f(x) = \frac{1}{2x_0} \frac{\gamma}{(1 + |x|/x_0)^{1+\gamma}}, \quad 0 < \gamma < 1, \quad (12)$$

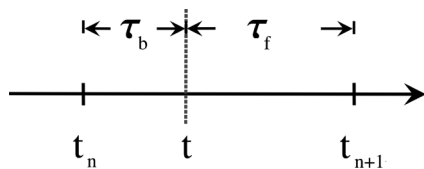


FIG. 2. Backward and forward recurrence times. Given a measurement time  $t$ , the backward recurrence time  $\tau_b$  is the time elapsed since the time  $t_n$  the last event took place. The forward recurrence time  $\tau_f$  is the time span between  $t$  and the time  $t_{n+1}$  at which the next renewal will take place.

for the jump-length distribution in the jump-first model. Note that our final results are not sensitive to the specific small  $\tau$  or  $x$  behavior. The power-law tails completely determine the long-time behavior which is rooted in the generalized central limit theorem, see, for example, Ref. [13]. Thus our results are valid for the general class of waiting-time or jump-length pdfs that have the same asymptotic limit as Eq. (11) or Eq. (12), respectively.

Via the coupling relations (4) and (5), the Eqs. (11) and (12) fully determine also the step lengths of the wait-first and time intervals of the jump-first model, respectively. Thus in the wait-first case the full coupled jump pdf is

$$K_w(x,\tau) = \psi(\tau)f(x|\tau) = \frac{1}{\tau_0} \frac{\gamma}{(1 + \tau/\tau_0)^{1+\gamma}} \delta(|x| - v_0\tau), \quad (13)$$

from which we calculate the effective jump-length pdf,

$$f_w(|x|) = \int_0^\infty \Psi(x,\tau) d\tau = \frac{1}{v_0\tau_0} \frac{\gamma}{[1 + |x|/(v_0\tau_0)]^{1+\gamma}}, \quad (14)$$

which corresponds exactly to (12) if we set  $x_0 = v_0\tau_0$ . An analogous derivation applies for the jump-first model, so indeed Eqs. (4) and (5) together with (11) and (12) yield the same effective jump-length and waiting-time distributions. Thus  $f_w(|x|) = \psi(\tau)|_{\tau=|x|}$  and  $\psi_f(\tau) = f(|x|)|_{|x|=\tau}$  for  $x_0 = v_0\tau_0$ , which allows us to compare between the two jump models. The construction of the simple Lévy walk with two velocity states  $h(v) = 1/2[\delta(v - v_0) + \delta(v + v_0)]$  such that its steps all end in the same points in time and space as in the jump models requires us to choose the same  $v_0$  for all models. Later we will also see what changes in more complicated velocity models with distributed velocities. The resultant (effective) waiting-time pdfs of all these models lack a typical time scale since the mean waiting time diverges, and hence the overall motion of the particle will be governed by a few very large (of the order of the observation time) persistence time intervals during which the particle's state of motion does not change. Therefore this regime is referred to as the ballistic one [10,36].

### B. Fourier-Laplace inversion in the ballistic scaling regime

When stating that the propagator of a random-walk model has the ballistic scaling we imply that it can be written in the following form:

$$G(x,t) \cong \frac{1}{t} \Phi\left(\frac{x}{t}\right), \quad t \rightarrow \infty, \quad (15)$$

where  $\Phi$  is the scaling function. In Fourier-Laplace space this would correspond to a similar relation,

$$G(k,s) = \frac{1}{s} g\left(\frac{ik}{s}\right). \quad (16)$$

For the Fourier-Laplace inversion of this expression we will follow a procedure similar to that given, e.g., in Ref. [37]. By using the characteristic function and the definitions of the integral transforms we can write (see Appendix D)

$$G(k,s) = \int_0^\infty e^{-st} \langle e^{-ikX} \rangle dt = \frac{1}{s} \left\langle \frac{1}{1 + \frac{ik}{s} Y} \right\rangle. \quad (17)$$

Here angular brackets denote the averaging with respect to a random variable  $X$  which has a pdf  $P(X)$ ,

$$\langle F(X) \rangle = \int_{-\infty}^{\infty} F(X)P(X)dX. \quad (18)$$

In our case,  $X$  is the coordinate of the particle at time  $t$  and therefore  $P(X) = G(X,t)$ . In addition, we introduced a scaled variable  $Y = X/t$  to obtain the second line of Eq. (17). Now by comparing Eqs. (17) and (16) we can identify the scaling function  $g$  in Fourier-Laplace space as:

$$g(\xi) = \left\langle \frac{1}{1 + \xi Y} \right\rangle; \quad \xi \equiv \frac{ik}{s}. \quad (19)$$

We use the definition  $\Phi(y) = \langle \delta(y - Y) \rangle$  and the Sokhotsky-Weierstrass theorem [38] to write

$$\begin{aligned} \Phi(y) &= \langle \delta(y - Y) \rangle = -\frac{1}{\pi} \lim_{\epsilon \rightarrow 0} \text{Im} \left\langle \frac{1}{y - Y + i\epsilon} \right\rangle \\ &= -\frac{1}{\pi} \lim_{\epsilon \rightarrow 0} \text{Im} \left[ \frac{1}{y + i\epsilon} \left\langle \frac{1}{1 - \frac{Y}{y + i\epsilon}} \right\rangle \right]. \end{aligned}$$

Finally, if we compare the above formula with Eq. (19), we obtain the recipe to find the analytical expression of the scaling function  $\Phi(y)$  if its counterpart in Fourier-Laplace space  $g(\xi)$  is known:

$$\Phi(y) = -\frac{1}{\pi} \lim_{\epsilon \rightarrow 0} \text{Im} \left[ \frac{1}{y + i\epsilon} g \left( -\frac{1}{y + i\epsilon} \right) \right]. \quad (20)$$

A similar method was used before in Ref. [37] for the inversion of a double Laplace transform. Here it is generalized to the case of time and two-sided space variables (as in Ref. [39]). Below we demonstrate how it works in practice.

## IV. RESULTS FOR JUMP MODELS

### A. Two-sided jump models

We start with general analytical expressions for the propagators of the jump models Eqs. (8) and (9), use the simple coupling relations Eqs. (4) and (5), and proceed with the asymptotic analysis. For a waiting-time distribution of the form as in Eq. (11) in the long-time limit, its expansion in Laplace space is given by [and similarly for the jump-length pdf Eq. (12) in Fourier space]

$$\psi(s) \simeq 1 - \tau_0^\gamma \Gamma(1 - \gamma) s^\gamma. \quad (21)$$

After some algebra (see Appendix B) we find for the propagators in the Fourier-Laplace domain in the small- $k$  and - $s$  limits

$$G_j(k,s) = \frac{1}{s} \left[ 1 - \frac{(ikv_0)^\gamma + (-ikv_0)^\gamma}{(s + ikv_0)^\gamma + (s - ikv_0)^\gamma} \right] \quad (22)$$

and

$$G_w(k,s) = \frac{1}{s} \frac{2s^\gamma}{[(s - ikv_0)^\gamma + (s + ikv_0)^\gamma]}. \quad (23)$$

We indeed see that these expressions assume the scaling form as in Eq. (16), from which we identify the scaling functions

$$g_j(\xi) = 1 - \frac{(-\xi)^\gamma + (\xi)^\gamma}{(1 - \xi)^\gamma + (1 + \xi)^\gamma} \quad (24)$$

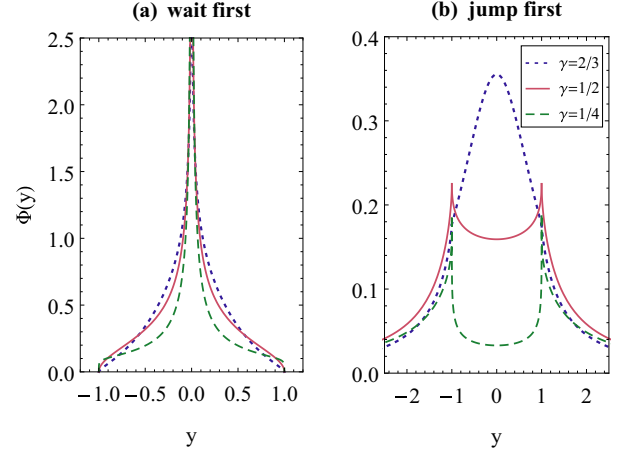


FIG. 3. (Color online) Propagators of two jump models in the ballistic scaling regime. The rescaled propagators for (a) the wait-first and (b) the jump-first models from Eqs. (27) and (26) are shown for different values of the exponent  $\gamma$  determining the power-law tail of the waiting-time and jump-length distributions.

and

$$g_w(\xi) = \frac{2}{(1 - \xi)^\gamma + (1 + \xi)^\gamma} \quad (25)$$

with  $\xi = iv_0k/s$  so the scaling variable becomes  $y = x/(v_0t)$ . This allows us again to perform the Fourier-Laplace inversion in the scaling regime. By Eqs. (20), (22), and (23) we find the scaling solutions in original space-time domain:

$$\begin{aligned} \Phi_j(y) &= \frac{\sin[\pi\gamma]}{\pi} y^{-1} \\ &\times \begin{cases} \frac{\text{sign}y}{|y+1|^\gamma + |y-1|^\gamma} & 1 \leq |y| < \infty \\ \frac{|y+1|^\gamma - |y-1|^\gamma}{|y+1|^{2\gamma} + |y-1|^{2\gamma} + 2|y+1|^\gamma |y-1|^\gamma \cos[\pi\gamma]} & 0 \leq |y| < 1 \end{cases} \end{aligned} \quad (26)$$

$$\begin{aligned} \Phi_w(y) &= \frac{2 \sin[\pi\gamma]}{\pi} |y|^{\gamma-1} \\ &\times \begin{cases} 0 & 1 \leq |y| < \infty \\ \frac{(1-|y|)^\gamma}{|y+1|^{2\gamma} + |y-1|^{2\gamma} + 2|y+1|^\gamma |y-1|^\gamma \cos[\pi\gamma]} & 0 \leq |y| < 1 \end{cases} \end{aligned} \quad (27)$$

where  $y = x/(v_0t)$  is the scaling variable (see Fig. 3). We also find from Eq. (23) a mean-squared displacement (MSD)  $\langle x^2 \rangle_w = (1 - \gamma)\gamma v_0^2 t^2 / 2$  or in terms of the scaling variable  $\langle y^2 \rangle_w = (1 - \gamma)\gamma / 2$ . Although the pdf for the jump-first model scales ballistically, it does not possess a finite MSD. This is to be expected, since the variance of the jump length diverges and the jump is performed at the beginning of a waiting time—the last jump can be very large when the corresponding last waiting time is far from being completed.

### B. One-sided jump models

The reason for the remarkable shape differences of the scaled densities for the different models (see Fig. 3) becomes immediately clear if we consider the following simplified

example. In what follows we allow for jumps only in the positive direction and indicate this in the scaling functions by a superscript “+.” The scaling functions become

$$g_j^+(\xi) = 1 - \frac{\xi^\gamma}{(1+\xi)^\gamma}, \quad g_w^+(\xi) = \frac{1}{(1+\xi)^\gamma}.$$

Thus, the one-sided scaling solutions are

$$\Phi_j^+(y) = \begin{cases} \frac{\sin[\pi\gamma]}{\pi} y^{-1}(y-1)^{-\gamma} & 1 < y < \infty \\ 0 & -\infty \leq y \leq 1 \end{cases}, \quad (28)$$

$$\Phi_w^+(y) = \begin{cases} 0 & 1 < y < \infty \\ \frac{\sin[\pi\gamma]}{\pi} (1-y)^{-\gamma} y^{\gamma-1} & -\infty \leq y \leq 1 \end{cases}, \quad (29)$$

as shown in Fig. 4. The MSD of the jump-first model again diverges. For the one-sided wait-first model  $\langle x^2 \rangle_w = (1+\gamma)\gamma v_0^2 t^2/2$  and thus  $\langle y^2 \rangle_w = (1+\gamma)\gamma/2$ , or  $\text{var}(y)_w = (1-\gamma)\gamma/2$ , as  $\langle y \rangle_w = \gamma$ . The propagators of the one-sided jump models are closely related to the distributions of forward and backward recurrence times  $\tau_f$  and  $\tau_b$ , i.e., the time interval from the measurement time to the next renewal and the time interval that passed since the last renewal, respectively (see Fig. 2). The positions  $x$  in the jump- and wait-first models are  $x^{(j)} = v_0(t + \tau_f)$ ,  $x^{(w)} = v_0(t - \tau_b)$  and thus

$$y^{(j)} = 1 + \frac{\tau_f}{t}, \quad (30)$$

$$y^{(w)} = 1 - \frac{\tau_b}{t}. \quad (31)$$

Indeed, the forward and backward recurrence time scaling distributions of the variables  $y^{(f)} = \tau_f/t$  and  $y^{(b)} = \tau_b/t$  are obtained by performing the above transformations Eqs. (30) and (31) of the scaling variables  $y$  in Eqs. (28) and (29), respectively (see also Refs. [37,40]). This example demonstrates strikingly that the difference between the models comes into effect only through the last renewal period.

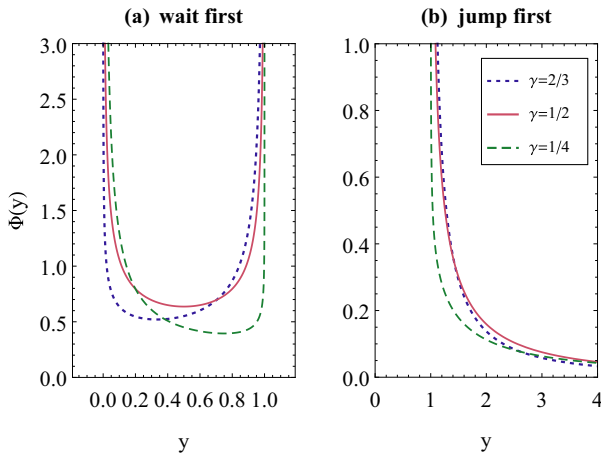


FIG. 4. (Color online) One-sided jump models. In this particular case only jumps to the right are allowed. One-sided wait-first (a) and jump-first models (b) [Eqs. (29) and (28)] are shown for different values of the power-law tail exponent  $\gamma$  governing the flight and jump-length distributions. These results are related to the statistics of the backward and forward recurrence times, as discussed in the text.

## V. RESULTS FOR THE VELOCITY MODELS

The propagator for the velocity model Eq. (10) can be rewritten as

$$G_v(k,s) = \frac{\int_{-\infty}^{\infty} dv \Psi(s+ikv)h(v)}{1 - \int_{-\infty}^{\infty} dv \psi(s+ikv)h(v)}, \quad (32)$$

where the  $\Psi(s+ikv)$  and  $\psi(s+ikv)$  are Laplace transforms and the shift theorem was used (see Appendix C). This result is exact, provided both integrals in Eq. (32) converge. In the ballistic regime  $0 < \gamma < 1$  we use the expansion given in Eq. (21) to obtain the asymptotic version of this result,

$$G_v(k,s) = \frac{1}{s} \frac{\int_{-\infty}^{\infty} (1+ikv/s)^{\gamma-1} h(v) dv}{\int_{-\infty}^{\infty} (1+ikv/s)^\gamma h(v) dv}. \quad (33)$$

By comparing it with the scaling form of Eq. (16) we obtain

$$g_v(\xi) = \frac{\int_{-\infty}^{\infty} (1+\xi v)^{\gamma-1} h(v) dv}{\int_{-\infty}^{\infty} (1+\xi v)^\gamma h(v) dv}. \quad (34)$$

Finally, performing the inversion in the scaling regime according to Eq. (20) yields

$$\Phi_v(y) = -\frac{1}{\pi} \lim_{\epsilon \rightarrow 0} \text{Im} \frac{\int_{-\infty}^{\infty} (y+i\epsilon-v)^{\gamma-1} h(v) dv}{\int_{-\infty}^{\infty} (y+i\epsilon-v)^\gamma h(v) dv}. \quad (35)$$

We should note that the problem of finding the propagator in the velocity model corresponds to the problem of time averaging the position of a subdiffusing particle subject to an external binding potential as investigated in detail in Ref. [39]: Indeed, we can view the velocity model as a decoupled CTRW in velocity space, and the inference of the particle position requires an integration over time. The scaled (here  $v_0 = 1$ ) position  $y = x/t$  of the single particle after a time  $t$ , provided it started at  $t_0 = 0$ ,  $x_0 = 0$  is given by

$$y(t) = \frac{1}{t} \int_0^t v(t') dt'. \quad (36)$$

Thus, for the time-averaged CTRW,  $h(v)$  corresponds to the Boltzmann equilibrium or steady-state distribution in space [39].

Let us now furnish the above result with some examples. We start with the two-state velocity pdf  $h(v) = [\delta(v-v_0) + \delta(v+v_0)]/2$ . By repeating the same sequence of steps as for the jump models we arrive at

$$g_v(\xi) = \frac{(1-\xi)^{\gamma-1} + (1+\xi)^{\gamma-1}}{(1-\xi)^\gamma + (1+\xi)^\gamma}, \quad (37)$$

$\xi = ikv_0/s$ . With Eq. (20) the scaling form of the propagator is found to be the Lamperti distribution [41],

$$\Phi_v(y) = \frac{\sin \pi \gamma}{\pi} \times \frac{|y-1|^\gamma |y+1|^{\gamma-1} + |y+1|^\gamma |y-1|^{\gamma-1}}{|y-1|^{2\gamma} + |y+1|^{2\gamma} + 2|y-1|^\gamma |y+1|^\gamma \cos \pi \gamma} \quad (38)$$

where  $y = x/(v_0 t)$  and  $|y| < 1$  and  $\langle y^2 \rangle = (1-\gamma)$ . This distribution plays a role, for example, in the prediction of

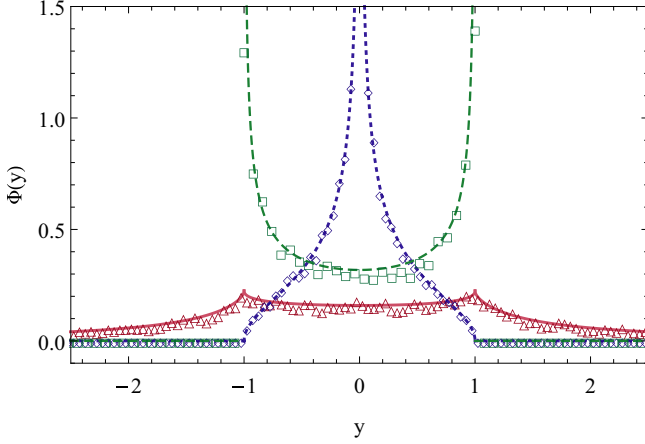


FIG. 5. (Color online) Theory and simulations for the wait-first model [Eq. (27)] (solid line, triangles, red), the jump-first model [Eq. (26)] (dotted line, diamonds, blue) and the two-state velocity model Eq. (38) (dashed line, squares, green).  $\gamma = 1/2$ , scaling variable  $y = x/(v_0 t)$ .

the time-averaged intensity of the light emitted by a blinking quantum dot [9]. For  $\gamma = 1/2$  this scaling distribution assumes a particularly simple form,

$$\Phi_v(y) = \frac{1}{\pi(1-y^2)^{1/2}}, \quad |y| < 1, \quad (39)$$

the well-known arcsine distribution [40]. It is instructive to compare the propagator of this type of Lévy walk with those of the two jump models. As is clear from Fig. 1, the trajectory of the walk passes through the same end points as both jump models, yet it does it by a different path in the  $(x, t)$  plane. As a result, the shape of the propagator is very distinct, see Fig. 5. As before, the origin of the difference is in the last unfinished step: In the case of the corresponding one-sided walk, i.e. the walk with just one velocity  $h(v) + \delta(v - v_0)$ , the position of the particle is given by a simple  $x^{(v)} = v_0 t$ , different from both jump models. We also use Fig. 5 to compare our analytical results with direct numerical simulations of random-walk models which show excellent agreement. Figure 5 clearly demonstrates that the particles spread further in the jump-first model if compared with the velocity- and wait-first models, the latter being the slowest process.

The distinct feature of the velocity model is the ability to include the velocity distribution of the random walking particles. Below we show how different velocity pdfs change the scaling shape of the corresponding propagator. For illustration, in addition to the two-state velocity pdf, we chose a uniform velocity distribution on finite-interval, Gaussian, and Cauchy distributions.

For the uniform velocity pdf between  $\pm v_0$ ,  $\theta(v_0 - |v|)/(2v_0)$ , where  $\theta$  is the Heaviside step function, we find with  $\xi = v_0 i k/s$

$$g_v(\xi) = \frac{(1+\gamma)}{\gamma} \frac{((1-\xi)^\gamma - (1+\xi)^{1-\gamma})}{(1-\xi)^{1+\gamma} - (1+\xi)^{1+\gamma}} \quad (40)$$

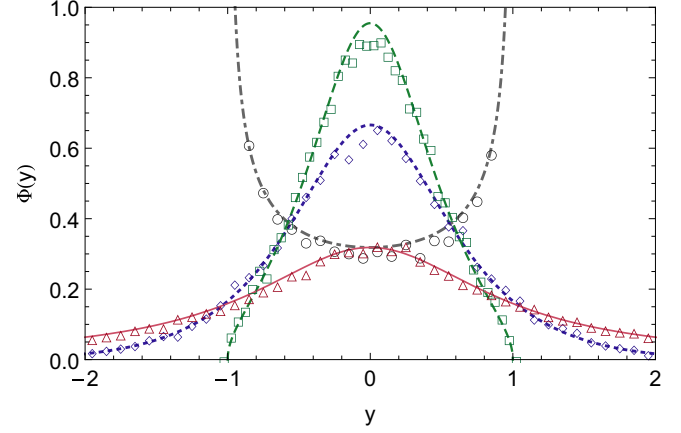


FIG. 6. (Color online) Scaling functions of the random walks with random velocities model. Results for four different velocity pdfs of the walking particles are depicted: two-state velocity  $v = \pm v_0$  [Eq. (39)] (dash-dot, circles, gray), uniform on an interval [Eq. (42)]  $[-v_0, v_0]$  (dashed, squares, green), Gaussian [Eq. (35)] (dotted, diamonds, blue), and Cauchy [Eq. (45)] (full line, triangles, red);  $\gamma = 1/2$ . The result for the Gaussian velocity pdf was obtained using MATHEMATICA. Theory and simulations nicely match without fitting.

and

$$\Phi_v(y) = \frac{2(1+\gamma) \sin \pi \gamma}{\pi \gamma} \times \frac{(1-y^2)^\gamma}{(1-y)^{2+2\gamma} + (1+y)^{2+2\gamma} + 2(1-y^2)^{1+\gamma} \cos \pi \gamma}, \quad (41)$$

with the MSD  $\langle y^2 \rangle = 1/3(1-\gamma)$ . For  $\gamma = 1/2$  it reduces to a very simple expression,

$$\Phi_v(y) = \frac{3\sqrt{1-y^2}}{\pi(1+3y^2)}, \quad (42)$$

shown in Fig. 6 (dashed, squares, green). As we see, similarly to the Lévy-walk case with two velocity states, the propagator is bounded by ballistic fronts corresponding to the maximal possible speed. However, it has more of a bell-shaped profile, unlike the shape of the single-speed Lévy walk with its distinct infinite peaks at  $|y| = 1$ .

For a Gaussian velocity pdf  $h(v) = (2\pi v_0^2)^{-1/2} \exp[-v^2/(2v_0^2)]$  we get a more involved expression,

$$g_v(\xi) = \frac{\int_{-\infty}^{\infty} [1 + \xi v]^{-1/2} \exp[-\frac{v^2}{2v_0^2}] dv}{\int_{-\infty}^{\infty} [1 + \xi v]^{1/2} \exp[-\frac{v^2}{2v_0^2}] dv}. \quad (43)$$

For  $\gamma = 1/2$ , the corresponding Eq. (35) can be solved (for example, in MATHEMATICA) and expressed in terms of hypergeometric (or Kummer's) functions of the first and second kinds, see Fig. 6 (dotted, diamonds, blue). Since the Gaussian pdf, in principle, allows for infinite speeds, the profile of the propagator this time is unbounded. Still, the MSD remains finite,  $\langle y^2 \rangle = 1 - \gamma$ . Indeed, if the second moment of a symmetric  $h_{sc}(v) = h(v/v_0)/v_0$  exists, we always have  $\langle y^2 \rangle = (1-\gamma)\langle v^2 \rangle/v_0^2$ , see also Ref. [39].

A very special situation is induced by Cauchy-distributed velocities,  $h(v) = 1/\{\pi v_0[1 + (v/v_0)^2]\}$ . It was shown in Ref. [28] that in this case the flight-time distribution, in particular the value of  $\gamma$ , has no effect on the resulting propagator, which in turn is also Cauchy. To show this, let us consider the exact answer for the velocity model as in Eq. (10) and substitute the Fourier transform of the Cauchy velocity distribution:  $h(k\tau) = \exp(-v_0|k|\tau)$ . After simple algebra, and without prescribing the particular form of  $\psi(\tau)$ , we arrive at:

$$G_v(k, s) = \frac{1}{s + v_0|k|}. \quad (44)$$

One can immediately recognize that the inverse Laplace and Fourier transform of Eq. (44) will again lead to the Cauchy distribution:

$$G_v(x, t) = \frac{v_0 t}{\pi(v_0^2 t^2 + x^2)}. \quad (45)$$

Therefore the scaling function, which we plot in Fig. 6 (full line, triangles, red), has the simple form  $\Phi_v(y) = [\pi(1 + y^2)]^{-1}$ , and its MSD clearly diverges. For such a simple answer for the propagator in Fourier-Laplace space, Eq. (44), the application of the proposed inversion method becomes somewhat redundant; however, it can be demonstrated that it works here as well. To conclude this section we note that the model of random walks is very sensitive to the shape of the velocity distribution which gets reflected in the profile of the asymptotic density. This was noticed before [39], as well as a similar phenomenon in the sub-ballistic, superdiffusive regime [27]. However, in the subballistic case the effect was much weaker, as it appeared only at the far tails of the distribution, whereas in the ballistic regime it dominates the whole propagator.

## VI. DISCUSSION

We considered the long-time scaling limit of the density profiles of particles for a large class of one-dimensional random walks that operate in the ballistic regime, which implies a scaling variable  $y \sim x/t$ . Depending on the model, these densities differ strikingly. It is important to note that especially the last renewal period plays a crucial role with regard to these differences. If we compare the jump models and the simple velocity model with constant speed where at the renewal only the direction of motion is chosen, we find that exactly at the instant of a renewal the jump-first, wait-first, and the simple velocity models are the same (Fig. 1). Thus they differ only by their last renewal interval, and this is the origin of the difference between their densities.

For both the one- and two-sided wait-first models the propagator is restricted to a finite interval of the scaling variable,  $y \in (0, 1)$  and  $y \in [-1, 1]$ , respectively, since the particles can never overcome the front  $|x| = v_0 t$ . In contrast to that, in the one-sided jump-first model the particles jump further ahead whenever the front catches up with them, therefore  $y \in (1, \infty)$ . In the two-sided jump-first model we have  $y \in (-\infty, \infty)$ . The propagators of both jump-first models exhibit heavy tails (Figs. 4 and 3, right panels) which renders them somewhat unphysical. Nevertheless, they can serve as an impressive demonstration of the large effect of the final jump.

Whether the scaled propagators of the velocity model have a heavy tail or live on a finite domain depends directly on the underlying velocity pdfs which can exhibit heavy tails or are constricted to a finite interval. We explicitly calculated the scaled densities for some velocity and jump models, for which we found excellent agreement with the results of direct Monte Carlo simulations of the respective processes. Although we considered  $\delta$ -function-like coupling between the jump distance and time it takes, the method that we suggested only requires the existence of the ballistic scaling. Therefore it can in principle be applied to other, distributed, couplings as long as they lead to the ballistic regime. The mathematical machinery behind the method is specific to the ballistic regime, and it will be necessary to develop other approaches for different scaling regimes. We believe that the analytical results presented here provide an important step in our quantitative understanding of random walks and will facilitate the implementation of these random-walk models in physics and other interdisciplinary applications.

## ACKNOWLEDGMENTS

M.S. was supported by the Deutsche Forschungsgemeinschaft within the Emmy Noether program (Grant No. Schm2657/2). E.B. thanks the Israel Science Foundation and the Max Planck Institute for the Physics of Complex Systems.

## APPENDIX A: JUMP MODELS: PROPAGATOR IN THE FOURIER-LAPLACE DOMAIN

Fourier-Laplace transformation of Eq. (1) yields

$$Q_\alpha(k, s) = K_\alpha(k, s)Q_\alpha(k, s) + 1, \quad (A1)$$

$$Q_\alpha(k, s) = \frac{1}{1 - K_\alpha(k, s)},$$

where  $K_j(k, s) = \mathcal{FL}\{f(x)\psi(\tau|x)\}$  and  $K_w(k, s) = \mathcal{FL}\{f(x|\tau)\psi(\tau)\}$ . The Fourier-Laplace transform is defined as  $\mathcal{FL}\{\cdot\} = \int_{-\infty}^{\infty} dx \int_0^{\infty} dt e^{-ikx} e^{-st}(\cdot)$ . For Eqs. (2) and (3) we have

$$p_w(k, s) = \mathcal{L}\{\Psi(\tau)\}Q_w(k, s), \quad (A2)$$

$$p_j(k, s) = \mathcal{FL}\{f(x)\Psi(\tau|x)\}Q_w(k, s). \quad (A3)$$

Inserting (A1) results in Eqs. (8) and (9).

## APPENDIX B: JUMP MODELS: FORMAL SCALING SOLUTION

Equations (8) and (9) simplify due to the shift theorem for linear coupling, Eqs. (4) and (5):

$$G(k, s) = \frac{F(k, s)}{1 - \mathcal{F}\left\{\exp\left[-s\frac{|x|}{v}\right]f(|x|)\right\}}, \quad (B1)$$

where  $f$  is the coupling function between jump length and waiting time. For the jump-first model,

$$F_j(k, s) = \mathcal{F}\left\{\frac{f(|x|)}{s}\left(1 - \exp\left[-s\frac{|x|}{v}\right]\right)\right\}, \quad (B2)$$

and

$$F_w(k, s) = \frac{1 - \psi(s)}{s} \quad (\text{B3})$$

for the wait-first model. With Eq. (21) the denominator in (B1) becomes

$$\begin{aligned} & 1 - \int_{-\infty}^0 e^{\frac{sx}{v_0}} \frac{1}{2v_0} \psi\left(-\frac{x}{v_0}\right) e^{-ikx} dx \\ & - \int_0^{\infty} e^{-\frac{sx}{v_0}} \frac{1}{2v_0} \psi\left(\frac{x}{v_0}\right) e^{-ikx} dx \\ & \simeq \frac{\tau_0^\gamma \Gamma(1 - \gamma)}{2} [(s + ikv_0)^\gamma + (s - ikv_0)^\gamma]. \end{aligned} \quad (\text{B4})$$

Correspondingly, we have for Eq. (B2)

$$\begin{aligned} & \frac{1}{s} \left[ \int_{-\infty}^0 \frac{1}{2v_0} \psi\left(-\frac{x}{v_0}\right) (1 - e^{\frac{sx}{v_0}}) e^{-ikx} dx \right. \\ & \left. + \int_0^{\infty} \psi\left(\frac{x}{v_0}\right) (1 - e^{-\frac{sx}{v_0}}) e^{-ikx} dx \right] \\ & \simeq \frac{1}{s} \left[ 1 - \frac{\tau_0^\gamma \Gamma(1 - \gamma)}{2} [(+ikv_0)^\gamma + (-ikv_0)^\gamma] - 1 \right. \\ & \left. + \frac{\tau_0^\gamma \Gamma(1 - \gamma)}{2} [(s + ikv_0)^\gamma + (s - ikv_0)^\gamma] \right] \end{aligned} \quad (\text{B5})$$

and for Eq. (B3)

$$\frac{1 - \psi(s)}{s} \simeq \frac{1}{s} \tau_0^\gamma \Gamma(1 - \gamma) s^\gamma. \quad (\text{B6})$$

Inserting this back into Eq. (B1) yields Eqs. (22) and (23), respectively.

### APPENDIX C: PROPAGATOR IN THE VELOCITY MODEL

Let us write explicitly the numerator in the fraction of Eq. (10)

$$\begin{aligned} & \mathcal{L}\{\Psi(\tau)h(k\tau)\}(k, s) \\ & = \int_0^{\infty} d\tau \int_{-\infty}^{\infty} dv e^{-ik\tau v} e^{-s\tau} \Psi(\tau)h(v) \\ & = \int_{-\infty}^{\infty} dv \left( \int_0^{\infty} d\tau e^{-(s+ikv)\tau} \Psi(\tau)h(v) \right) \\ & = \int_{-\infty}^{\infty} dv \Psi(s + ikv)h(v). \end{aligned} \quad (\text{C1})$$

Analogously, for the denominator,

$$\begin{aligned} & 1 - \mathcal{L}\{\psi(\tau)h(k\tau)\}(k, s) \\ & = 1 - \int_{-\infty}^{\infty} dv \psi(s + ikv)h(v). \end{aligned} \quad (\text{C2})$$

Inserting this into Eq. (10) yields Eq. (32).

### APPENDIX D: FOURIER-LAPLACE TRANSFORM OF THE SCALING FUNCTION

Explicitly, the Fourier-Laplace transform of Eq. (15) is

$$\int_{-\infty}^{\infty} \int_0^{\infty} \exp[-ikx - st] \frac{1}{t} \Phi\left(\frac{x}{t}\right) dt dx. \quad (\text{D1})$$

Subsequent variable transformation leads to

$$\begin{aligned} & \int_{-\infty}^{\infty} \int_0^{\infty} \exp[-(iky + s)t] \Phi(y) dt dy \\ & = \int_{-\infty}^{\infty} \frac{\Phi(y)}{iky + s} dy = \frac{1}{s} \int_{-\infty}^{\infty} \frac{\Phi(y)}{\frac{ik}{s}y + 1} dy, \end{aligned} \quad (\text{D2})$$

which is equivalent to Eq. (17).

- 
- [1] K. Pfeilsticker, *J. Geophys. Res. Atmos.* **104**, 4101 (1999).
  - [2] E. Korobkova, T. Emonet, J. M. G. Vilar *et al.*, *Nature* **428**, 574 (2004).
  - [3] P. Barthelemy, J. Bertolotti, and D. S. Wiersma, *Nature* **453**, 495 (2008).
  - [4] F. Matthäus, M. S. Mommer, T. Curk, and J. Dobnikar, *PLoS ONE* **6**, e18623 (2011).
  - [5] Y. Sagi, M. Brook, I. Almog, and N. Davidson, *Phys. Rev. Lett.* **108**, 093002 (2012).
  - [6] D. A. Kessler and E. Barkai, *Phys. Rev. Lett.* **108**, 230602 (2012).
  - [7] A. Dechant, E. Lutz, D. A. Kessler, and E. Barkai, *Phys. Rev. X* **4**, 011022 (2014).
  - [8] Q. Baudouin, W. Guerin, and R. Kaiser, *Annu. Rev. Cold Atoms Mol.* **2**, 251 (2014).
  - [9] G. Margolin and E. Barkai, *Phys. Rev. Lett.* **94**, 080601 (2005).
  - [10] G. Margolin, V. Protasenko, M. Kuno, and E. Barkai, *J. Phys. Chem. B* **110**, 19053 (2006).
  - [11] D. Summers and R. Thorne, *Phys. Fluids B* **3**, 1835 (1991).
  - [12] H. Scher and M. Lax, *Phys. Rev. B* **7**, 4491 (1973).
  - [13] J.-P. Bouchaud and A. Georges, *Phys. Rep.* **195**, 127 (1990).
  - [14] R. Metzler and J. Klafter, *Phys. Rep.* **339**, 1 (2000).
  - [15] V. Zaburdaev, S. Denisov, and J. Klafter, [arXiv:1410.5100](https://arxiv.org/abs/1410.5100) [cond-mat.stat-mech].
  - [16] G. Zumofen and J. Klafter, *Phys. Rev. E* **47**, 851 (1993).
  - [17] M. F. Shlesinger, J. Klafter, and Y. M. Wong, *J. Stat. Phys.* **27**, 499 (1982).
  - [18] M. F. Shlesinger, B. J. West, and J. Klafter, *Phys. Rev. Lett.* **58**, 1100 (1987).
  - [19] P. Becker-Kern, M. M. Meerschaert, and H.-P. Scheffler, *Ann. Prob.* **32**, 730 (2004).
  - [20] A. Jurlewicz, P. Kern, M. M. Meerschaert, and H.-P. Scheffler, *Comput. Math. Appl.* **64**, 3021 (2012).
  - [21] T. Akimoto and T. Miyaguchi, *J. Stat. Phys.* **157**, 515 (2014).
  - [22] M. Magdziarz, W. Szczotka, and P. Żebrowski, *J. Stat. Phys.* **147**, 74 (2012).
  - [23] J. Liu and J. D. Bao, *Physica A* **392**, 612 (2013).
  - [24] M. Kotulski, *J. Stat. Phys.* **81**, 777 (1995).
  - [25] M. M. Meerschaert and E. Scalas, *Physica A* **370**, 114 (2006).
  - [26] P. Straka and B. I. Henry, *Stochast. Process. Appl.* **121**, 324 (2011).
  - [27] A. Rebenshtok, S. Denisov, P. Hänggi, and E. Barkai, *Phys. Rev. Lett.* **112**, 110601 (2014).

- [28] V. Zaburdaev, M. Schmiedeberg, and H. Stark, *Phys. Rev. E* **78**, 011119 (2008).
- [29] T. Geisel, J. Nierwetberg, and A. Zacherl, *Phys. Rev. Lett.* **54**, 616 (1985).
- [30] J. Klafter and I. M. Sokolov, *First Steps in Random Walks—From Tools to Applications* (Oxford University Press, Oxford, UK, 2011).
- [31] M. Schmiedeberg, V. Zaburdaev, and H. Stark, *J. Stat. Mech.* (2009) P12020.
- [32] E. Barkai and J. Klafter, *Lecture Notes in Physics*, Vol. 511 (Springer-Verlag, Berlin, 1998), p. 373.
- [33] E. W. Montroll and G. H. Weiss, *J. Math. Phys.* **6**, 167 (1965).
- [34] For comparison write  $k\tau = k^*$ , then  $n(k^*, s) = (\mathcal{L}\{\Psi(\tau)h(k^*)\}(k, s))/(1 - \mathcal{L}\{\psi(\tau)h(k^*)\}(k, s)) = ((1 - \psi(s))/s) (1/(1 - \psi(s)h(k^*)))n(t = 0, k^*)$ , where the initial condition is modified to account for the velocity pdf,  $n(t = 0, k^*, k) = h(k^*)\mathcal{F}_k\{n(t = 0, k)\}$ .
- [35] E. Barkai, E. Aghion, and D. A. Kessler, *Phys. Rev. X* **4**, 021036 (2014).
- [36] D. Froemberg and E. Barkai, *Eur. Phys. J. B* **86**, 331 (2013).
- [37] C. Godrèche and J. M. Luck, *J. Stat. Phys.* **104**, 489 (2001).
- [38] Sokhotsky-Weierstrass theorem:
- $$\lim_{\epsilon \rightarrow 0} \frac{1}{x \pm i\epsilon} = \frac{1}{x} \mp i\pi\delta(x),$$
- thus
- $$\mp \frac{1}{\pi} \text{Im} \lim_{\epsilon \rightarrow 0} \frac{1}{x \pm i\epsilon} = \delta(x).$$
- [39] A. Rebenshtok and E. Barkai, *J. Stat. Phys.* **133**, 565 (2008).
- [40] W. Feller, *An Introduction to Probability Theory and Its Applications*, Vol. 2 (Wiley, New York, 1966).
- [41] J. Lamperti, *Trans. Am. Math. Soc.* **88**, 380 (1958).